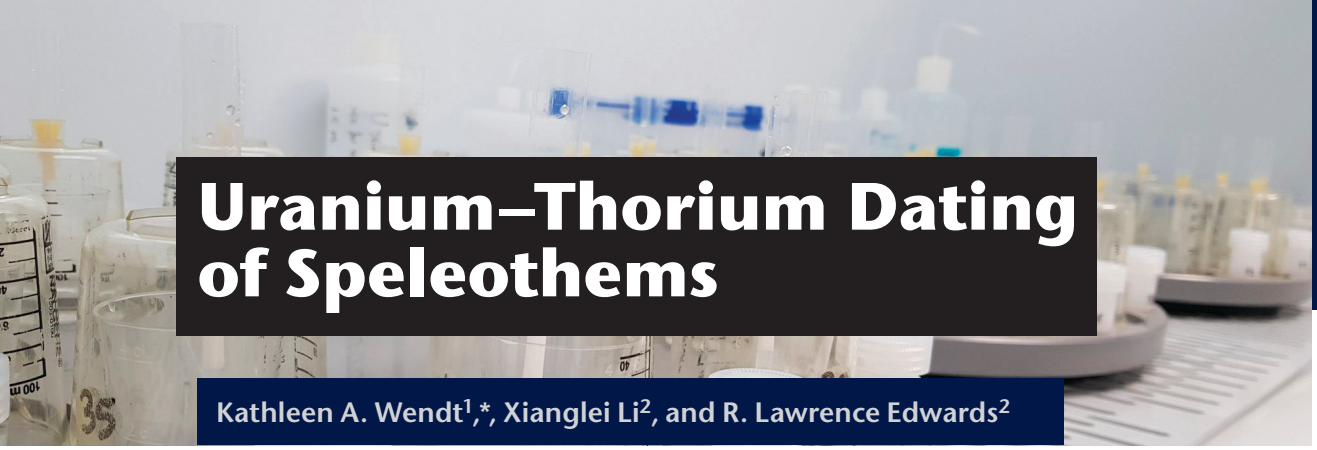

Uranium–Thorium Dating of Speleothems

Kathleen A. Wendt[1,*], Xianglei Li[2], and R. Lawrence Edwards[2]

1811-5209/21/0017-087$2.50 DOI: 10.2138/gselements.17.2.87

Speleothems are important timekeepers of Earth's climate history. A key advantage of speleothems is that they can be dated using U–Th techniques. Mass spectrometric methods for measuring U and Th isotopes has led to vast improvements in measurement precision and a dramatic reduction in sample size. As a result, the timing of past climate, environment, and Earth system changes can be investigated at exceptional temporal precision. In this review, we summarize the principles and history of U–Th dating of speleothems. Finally, we highlight three studies that use U–Th dated speleothems to investigate past changes to the Asian monsoon, constrain the timing of sociopolitical change in ancient civilizations, and develop a speleothem-based calibration of the ^{14}C timescale.

KEYWORDS: U–Th dating; ^{230}Th dating; U-series; speleothems; mass spectrometry

INTRODUCTION

A foundational pillar of the Quaternary sciences is the ability to date archives at an accuracy and precision that allows for meaningful interpretation (Richards and Andersen 2013). Well-preserved speleothems can be accurately dated using the uranium–thorium (U–Th) geochronometer in a time range from a few years to ~650,000 years. Uranium–thorium dating can be used to uncover an abundance of information contained in the isotopic, elemental, mineralogical, and molecular composition of speleothems. Speleothems are geographically widely distributed and often contain critical climate and environmental proxy information, such as past changes in temperature, precipitation, vegetation, and sea level. Some cave records can be correlated to records from marine sediments or ice cores, thereby establishing firm cave-based chronologies for a wealth of ocean and atmospheric data (e.g., Buizert et al. 2015; Cheng et al. 2016). Recently, speleothems have also been used to improve the precision of the radiocarbon dating calibration curve (Cheng et al. 2018; Reimer et al. 2020).

Uranium–thorium dating is based upon the ratios between three nuclides in the ^{238}U decay chain: ^{238}U, ^{234}U, and ^{230}Th. Carbonates precipitated from natural waters contain appreciable concentrations of U, but negligible concentrations of Th. With time, ^{230}Th in-grows through the decay of its parent isotope, ^{234}U. The degree of in-growth is the basis for the U–Th chronometer. Because ^{230}Th is itself radioactive, ratios among ^{230}Th, ^{234}U, and ^{238}U eventually reach steady-state values. The limit of the chronometer is reached when the isotopic composition of a sample is no longer distinguishable from an infinite-age sample. Using current technologies, the older age limit of the U–Th chronometer is about 650,000 years before present (650 ka).

Due to the extremely low concentrations of both ^{234}U and, especially, ^{230}Th (as low as a few parts in 10^{15}) the precision of U–Th ages is limited by analytical capabilities. Major breakthroughs in the development of analytical techniques (Edwards et al. 1987; Cheng et al. 2013) have increased the fraction of ^{230}Th and ^{234}U atoms that can be detected in a sample. Today, samples that are a few to 100 years old can be dated to a precision of one year. Under close to ideal circumstances, speleothems deposited at 10 ka can reach 2σ uncertainties as low as ±10 years, ±300 years at 130 ka, ±800 years at 200 ka, ±3 ky at 300 ka, ±8 ky at 400 ka, ±15 ky at 500 ka, and ±40 ky at 600 ka.

PRINCIPLES OF U–TH DATING

The ^{238}U Decay Chain

The decay rate, or activity (A), of any radioactive nuclide is defined as the number of decay events per unit time:

$$A = \frac{dN}{dt} = -\lambda N \quad (1)$$

where N is the number of atoms, λ is the decay constant for that nuclide, and t is time (Rutherford and Soddy 1902). Lambda (λ) is related to the half-life ($t_{1/2}$) of a nuclide by $t_{1/2} = \ln 2/\lambda$.

Uranium-238 (^{238}U) decays through a series of intermediate daughters to ^{206}Pb. Uranium-238 , which has a $t_{1/2}$ of 4.4683 ± 0.0048 × 10^9 years (Jaffey et al. 1971) decays by alpha emission to ^{234}Th ($t_{1/2}$ = 24.1 days), which decays by beta emission to ^{234}Pa ($t_{1/2}$ = 6.7 hours), which decays by beta emission to ^{234}U. Uranium-234 has a $t_{1/2}$ = 245,620 ± 290 years (Cheng et al. 2013) and decays by alpha emission to ^{230}Th, which has $t_{1/2}$ = 75,590 ± 110 (Cheng et al. 2013), which continues to decay through a series of intermediate daughters until ultimately reaching stable ^{206}Pb. Due to the short half-lives of ^{234}Th and ^{234}Pa in comparison to the timescales in question, both isotopes can be ignored in

1 University of Innsbruck
Institute of Geology
Innrain 52
6020 Innsbruck, Austria

* current address:
Oregon State University
College of Earth, Ocean, and Atmospheric Sciences
Corvallis, OR 97331, USA
E-mail: kathleen.wendt@oregonstate.edu

2 University of Minnesota
Department of Earth and Environmental Sciences
116 Church Street SE
Minneapolis, MN 55455, USA
E-mail: li000477@umn.edu, edwar001@umn.edu

carbonate dating applications. Thus, from a mathematical standpoint, we view ^{238}U as decaying directly to ^{234}U as follows:

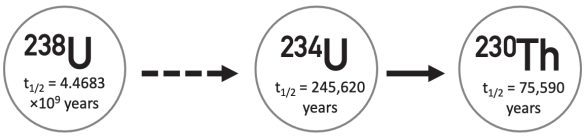

Disequilibrium Dating

Uranium–thorium dating is part of the U-series disequilibrium dating family. As with all disequilibrium dating schemes, the half-life of the parent nuclide is long relative to those of its intermediate daughter. If a system containing both parent and daughter remains closed, it will eventually approach a state of secular equilibrium (Rutherford and Soddy 1902; Bateman 1910), whereupon the activities of all nuclides in the series are equal (e.g., $N_1\lambda_1 = N_2\lambda_2 = N_3\lambda_3 = \ldots = N_n\lambda_n$, where N_1 is the number of atoms of nuclide 1, λ_1 is its decay constant, and the product $N_1\lambda_1$ is its activity). At secular equilibrium, the ratio of the activity of any of the daughters to the parent is unity (e.g., $N_1\lambda_1/N_2\lambda_2 = 1$). External processes that fractionate nuclides can disrupt this state of secular equilibrium, thereby shifting the activity ratios of the system away from unity (FIG. 1). If the system becomes closed again, it will return to unity over time through in-growth and decay. If the initial state of the system is known, one can calculate the time since the fractionation event occurred.

Chemical Properties of U and Th

The fractionation event in FIGURE 1 is made possible by the different chemical properties of U and Th. Under oxidizing conditions, U is highly soluble while Th is extremely insoluble. A striking illustration of the extreme solubility difference between U and Th is that surface sea waters have a $^{232}Th/^{238}U$ ratio on the order of 10^{-5} (Chen et al. 1986), which is ~10^5 lower than the bulk silicate Earth value of 3.8.

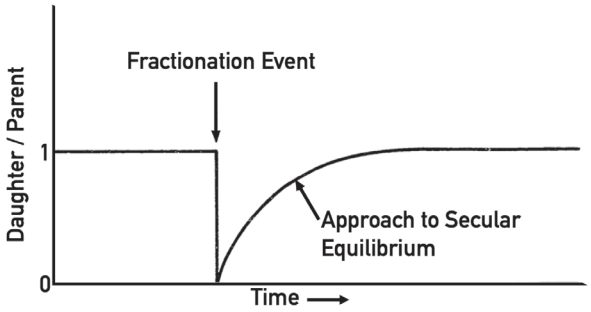

FIGURE 1 Conceptual diagram illustrating disequilibrium dating. The fractionation event represents the chemical fractionation of parent isotope from daughter isotope, resulting in disequilibrium. If the system once again becomes closed (e.g., by precipitation of a speleothem layer), the approach back to unity can be used to date the time the fractionation event occurred.

In the context of speleothems, the chemical fractionation of the parent U from the daughter Th occurs above the cave system. As meteoric water infiltrates through the soil column and bedrock, soluble U will dissolve in the passing waters while extremely low solubility Th will not (to any appreciable extent). Calcite that precipitates from these waters, if pure, will have a Th/U ratio close to zero. We will show below how the disequilibrium of $^{234}U/^{238}U$ and the concentration of initial ^{230}Th can complicate this idealized model.

The U–Th Dating Equation

The $^{230}Th/^{238}U$ activity ratio (denoted here as $[^{230}Th/^{238}U]_A$) in a speleothem will return to unity over time. This allows for the quantification of time since the system became closed, i.e., the time when the calcite precipitated. In a closed system, the extent to which the $[^{230}Th/^{238}U]_A$ has returned to unity is a function of time (t) and governed by the following equation:

$$\left[\frac{^{230}Th}{^{238}U}\right]_A = 1 - e^{-\lambda_{230}t} \quad (2)$$

A major shortcoming of Equation (2) is that it assumes that $[^{234}U/^{238}U]_A = 1$, whereas, in reality, the $[^{234}U/^{238}U]_A$ in most natural waters is >1 (Cherdyntsev et al. 1955). This may be surprising, because both ^{234}U and ^{238}U have identical chemical properties. Instead, U disequilibrium is thought to occur during the physical and chemical processes of weathering. The crystal lattice of the minerals that are in soils and bedrock holds ^{238}U. Over time, ^{238}U undergoes alpha-decay to short-lived ^{234}Th, which decays in a matter of days to ^{234}U. This energetic process can damage the bonds holding the ^{234}U in its site in a crystal lattice, leaving it susceptible to preferential leaching (Ivanovich and Harmon 1982). As a result, $[^{234}U/^{238}U]_A$ values are typically >1 in surface and ground waters, and <1 in soils and weathered rock. Groundwater $[^{234}U/^{238}U]_A$ can also vary over time and may be used as a climate or weathering proxy (e.g., Wendt et al. 2020).

Thus, because natural waters usually contain ^{234}U and ^{238}U in a state of disequilibrium, a second term must be added to Equation (2):

$$\left[\frac{^{230}Th}{^{238}U}\right]_A = 1 - e^{-\lambda_{230}t} + \left(\frac{\delta^{234}U_m}{1000}\right)\left(\frac{\lambda_{230}}{\lambda_{230}-\lambda_{234}}\right)\left(1 - e^{-(\lambda_{230}-\lambda_{234})t}\right) \quad (3)$$

where $\delta^{234}U = ([^{234}U/^{238}U]_A - 1) \times 1{,}000$ (Chen et al. 1986), and the subscript "m" indicates the measured value. This is the standard U–Th age equation, first derived by Kaufman and Broecker (1965). One can also calculate the initial $\delta^{234}U$ ($\delta^{234}U_0$) from the measured $\delta^{234}U$ and the age:

$$\delta^{234}U_m = \delta^{234}U_0 \cdot e^{-\lambda_{234}t} \quad (4)$$

A graphical representation of Equations (3) and (4) is shown in FIGURE 2. The axes are measured quantities $\delta^{234}U_m$ and $[^{230}Th/^{238}U]_A$, the latter corrected for initial ^{230}Th (see next section). The solution for age (t) is represented by a set of straight lines (Eqn. 3), and the solution for $\delta^{234}U_0$ values is represented by a set of curves (derived from Eqn. 4). By plotting the isotopic composition of a material on FIGURE 2, one can identify both the age of the material and the $\delta^{234}U_0$ value. Before the development of mass spectrometric techniques for U–Th dating (Edwards et al. 1987), this type of diagram was used infrequently and typically not in the context of carbonate dating, where the standard plot was one in which the x-axis was $[^{230}Th/^{234}U]_A$, instead of $[^{230}Th/^{238}U]_A$. Plotting $\delta^{234}U_m$ versus $[^{230}Th/^{238}U]_A$ has two key advantages: 1) curves of equal age are lines; 2) uncertainties (using mass spectrometric measurements) in the quantities that are plotted on the ordinate and abscissa are essentially uncorrelated. Because of these advantages, Richard Lawrence "Larry" Edwards popularized and described this plot in detail in the context of carbonate dating (Edwards 1988 and a set of subsequent papers by Edwards and colleagues, starting with Edwards et al. 1988). Hence, we call FIGURE 2 an "Edwards Diagram".

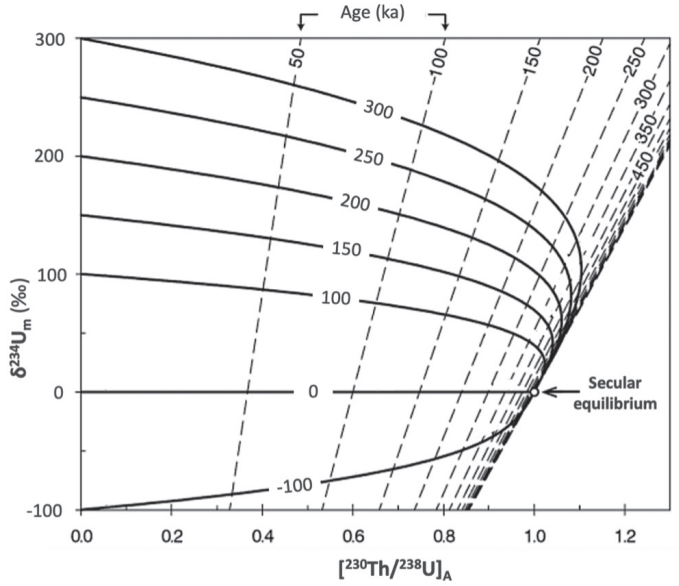

Figure 2 Plot of $\delta^{234}U_m$ vs. $[^{230}Th/^{238}U]_A$ ("Edwards Diagram"). Sloped dashed lines (ages in ka) represent solutions to the ^{230}Th age equation: the y-axis represents zero age (Eqn. 3); the curved contours are solutions to the $\delta^{234}U$ equation (Eqn. 4). Abbreviations: *A* = activity (i.e., radionuclide decay rate); m = measured value.

Initial and Closed System Conditions

Determining an accurate U–Th age requires prior knowledge of the initial ^{230}Th conditions. There are two sources of Th contamination. The first is hydrogenous Th which is transported by drip waters and incorporated into the calcite matrix upon precipitation. Due to the extreme insolubility of Th, however, the concentration of hydrogenous Th is often negligible. The second source is detrital material, such as clays, which can be cemented or occluded within a speleothem as it grows. In some cases, the concentration of detrital Th is significant and could bias U–Th ages without a proper correction.

The extent of Th contamination can be monitored by measuring ^{232}Th, which has the same chemical properties as ^{230}Th but is not an intermediate daughter in the ^{238}U decay chain. If the ^{232}Th concentration and the initial $^{230}Th/^{232}Th$ are known, the initial ^{230}Th concentration can be calculated. The initial $^{230}Th/^{232}Th$ can be estimated using one of several possible methods. First method: if the correction is small compared to analytical uncertainties, apply a generic correction (and apply a large uncertainty, e.g., ± 50% or 100%), e.g., the $^{230}Th/^{232}Th$ ratio of a material with a bulk Earth $^{232}Th/^{238}U$ ratio that is in secular equilibrium. Second method: apply a range of initial ratios commonly found in speleothems (e.g., Hellstrom et al 2006). Third method: employ an isochron technique by subsampling deposits of the same age that differ in $^{232}Th/^{238}U$. Fourth method: measure the $^{230}Th/^{232}Th$ of several detrital-rich laminae of a known age (e.g., Wang et al. 2001). In some cases, one can place bounds on initial $^{230}Th/^{232}Th$ using stratigraphic constraints in the form of development diagrams (e.g., Cheng et al. 2000). For details on these and other methods, see Richards and Dorale (2003).

Accurate U–Th ages also require that the system remain closed to postdepositional migration, including the addition or loss of U-series nuclides. A visual examination or chemical analysis of speleothems is necessary to check for signs of weathering or recrystallization, such as the conversion from aragonite to calcite, which may indicate that the sample has not remained a closed system. Another check for postdepositional migration is to test (i) if the U–Th ages from a sample are in stratigraphic order, or (ii) if the duration of growth phases can be replicated using alternative dating techniques, such as band counting.

METHODS OF U–TH DATING OF SPELEOTHEMS

History of Technical Developments

In the late 1890s, Henri Becquerel discovered that uranium salts can darken photographic plates. Shortly after, Marie Curie demonstrated that U and Th compounds ionized air and concluded that radioactivity was an atomic phenomenon. These early observations led to the discovery of ^{238}U, ^{235}U, and ^{232}Th decay chains, as well as the equations of radioactive production and decay (Rutherford 1902; Bateman 1910).

After an initial period of intense study, little was learned over the next three decades due to analytical difficulties in measuring small amounts of U and Th. This changed in 1941, when William Urry presented a method to determine U concentrations in natural samples. Barnes et al. (1956) were the first to apply U–Th dating to corals using alpha-decay counting techniques (α-spectrometry); this was later refined by Thurber et al. (1965), who accounted for the $^{234}U/^{238}U$ disequilibrium in natural waters. Although early applications of U–Th dating included measurements on marine sediment cores and cave calcites (e.g., Rosholt and Antal 1962), much of the focus was on fossil corals, which provide estimates on the timing of past sea levels.

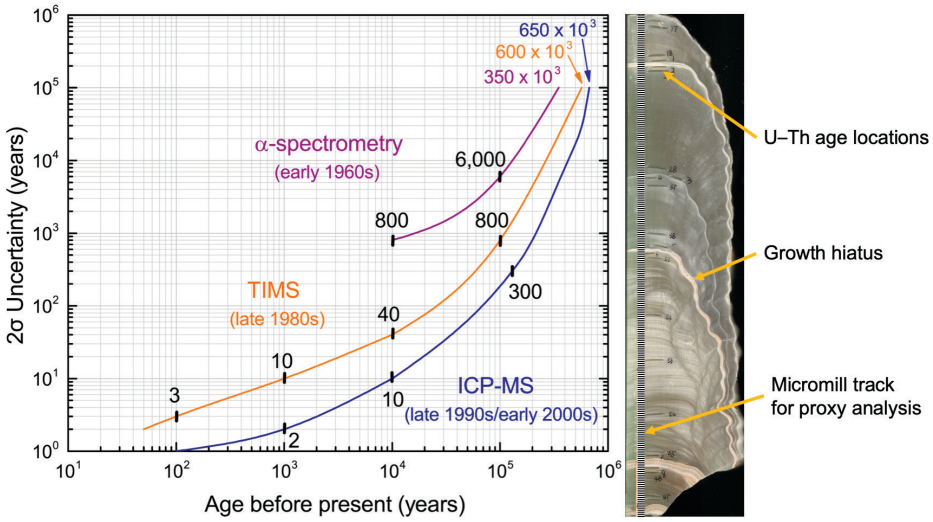

Figure 3 (**left**) Graphical representation of the ideal U–Th dating precision associated with three analytical methods as utilized for carbonates: alpha-spectrometry in the early 1960s; thermal ionization mass spectrometry (TIMS) in the 1980s; inductively coupled plasma mass spectrometry (ICP-MS) in the late 1990s and ICP-MS improvements in the early 2000s. Colored numbers indicate the oldest accessible ages with each technique. (**right**) Photo of the right side of a 27 cm stalagmite from Brazil that has been halved along its vertical growth axis. Labels indicate milling track for proxy analysis (striped bar indicating alternating growth layers) and subsampling holes for U–Th dating. Left and right panels are not directly related to each other.

Routine application of U–Th dating on speleothems gained prominence in the 1970s but was limited in terms of sample size and precision. These limitations were overcome with the development of mass spectrometric techniques for measuring ^{234}U (Chen et al. 1986) and ^{230}Th (Edwards et al. 1987), which dramatically improved precision, decreased sample size requirements by more than an order of magnitude, and extended the range of ^{230}Th dating to both younger and older time ranges. These improvements revitalized a field that has continued to expand dramatically more than three decades later. Initial mass spectrometric methods employed thermal ionization mass spectrometry (TIMS); since the 1980s, additional advancements in measurement precision have been made by using multi-collector inductively coupled plasma mass spectrometry (MC-ICP-MS) (e.g., Cheng et al. 2013).

Basis for Technical Improvements and Net Result

The greatest challenge in U–Th dating is detecting the extremely low natural abundances of ^{234}U and ^{230}Th, particularly ^{230}Th, which typically has abundances ranging from a few parts in 10^{15} (ppq) to several tens of parts in 10^{12} (ppt). Alpha-spectrometry is limited by the relatively long ^{230}Th half-life compared to laboratory counting times. Using this technique, one can detect ~1 out of 10^7 ^{230}Th atoms in a sample per week of counting time. The TIMS methods are limited by the fraction of ^{230}Th atoms that one can ionize in the mass spectrometer source (1 per 1,000), which is a four order magnitude of improvement on α-spectrometry. The MC-ICP-MS techniques are limited by the fraction of ions transmitted from the plasma into the source of the mass spectrometer, which is currently on the order of 1%–2% (e.g., Cheng et al. 2013), a further ten-fold improvement on the TIMS methods (FIG. 3, LEFT PANEL). These successive improvements have resulted in large reductions in sample size and improvements in age precision. Today, a typical sample-size ranges from a few tens of milligrams to several hundred milligrams. The photograph on the right side of FIGURE 3 shows the polished inner surface of a stalagmite cut along the growth axis and subsampled for U–Th dating and for oxygen isotopes (as a climate proxy).

OTHER U-SERIES DATING TECHNIQUES

Other geochronometers in the U-series disequilibrium family include uranium–protactinium (U–Pa) and uranium–uranium (U–U). The U–Pa geochronometer is based on the change in the $[^{231}Pa/^{235}U]_A$ ratio resulting from radioactive decay of ^{235}U to ^{231}Pa. Because Pa and Th have similar chemical properties, the systematics of U–Pa dating are analogous to those of U–Th dating. The U-Pa geochronometer (see Edwards et al. 1997) can be used to date carbonates deposited between 10 ka and 250 ka. The U–Pa geochronometer is applicable if the following conditions are met: (i) the initial ^{231}Pa–^{235}U ratio is zero, and (ii) the ^{231}Pa–^{235}U ratio has changed only by radioactive in-growth and decay.

The U–U geochronometer (Eqn. 4) is based on the change in the $[^{234}U/^{238}U]_A$ ratio, often expressed in delta notation, which occurs due to the radioactive decay of ^{238}U to ^{234}U. A significant limitation in U–U dating is the constraint of the initial value, $\delta^{234}U_0$, which exhibits a wide spatial and temporal variability in freshwater surface and ground waters (e.g., Wendt et al. 2020). As a result, U–U age uncertainties are often several orders of magnitude greater than U–Th dating. However, with a firm understanding of past source water $\delta^{234}U_0$, U–U dating represents a powerful geochronometer with a range that can reach beyond the older limits of U–Th dating (e.g., Li et al. 2021), potentially in excess of 2 million years.

The uranium–lead (U–Pb) geochronometer (see Woodhead et al. 2012) is based on the decay of ^{238}U and ^{235}U to the stable isotopes of ^{206}Pb and ^{207}Pb, respectively. The U–Pb geochronometer is frequently used to determine the age of speleothems older than ~1 Ma, extending back indefinitely hundreds of millions of years. The applicable timespan (on the young end) and precision of U–Pb dating is highly dependent on the concentrations of U and initial Pb in a speleothem. As with all other U-series dating techniques, the validity of a U–Pb age requires that the system has remained closed and that the initial conditions can be determined.

APPLICATIONS OF U–TH DATING OF SPELEOTHEMS

High-precision chronologies that have been derived from well-dated speleothems have yielded major discoveries over the last several decades. Here, we highlight three studies that applied U–Th dating methods to investigate the precise timing of three phenomena: Asian monsoon variability; the climate factors that contributed to the rise and fall of Chinese dynasties; past changes in atmospheric $^{14}C/^{12}C$.

Timing of the Asian Monsoon and Correlative Records

The seasonal cycle of solar heating over Asia gives rise to the Asian monsoon, a vast overturning system that transports heat and moisture across the Indian Ocean and the tropical west Pacific Ocean into the Indian subcontinent and Asia. Previous studies have shown that shifts in Chinese stalagmite $\delta^{18}O$ reflect changes in $\delta^{18}O$ of regional meteoric precipitation, which broadly anticorrelates with rainfall in the Asian monsoon system (see Johnson 2021

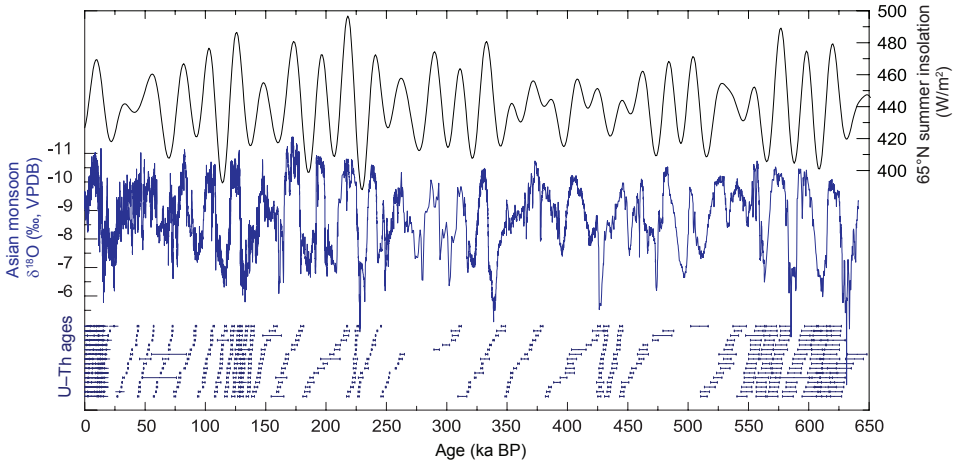

FIGURE 4 Asian monsoon variability over the last 640,000 years. (**TOP**) Northern Hemisphere summer insolation. (**MIDDLE**) Chinese speleothem $\delta^{18}O$ data. (**BOTTOM**) U–Th ages with associated 2σ uncertainties. Note that the $\delta^{18}O$ axis is reversed. Low (depleted) $\delta^{18}O$ are associated with periods of increased rainfall in the broad region affected by the Asian monsoon. Abbreviations: ka BP = thousands of years before present; VPDB = Vienna Pee Dee Belemnite (the international reference standard for carbonate oxygen isotopes). FIGURE MODIFIED FROM CHENG ET AL. (2016).

this issue). Cheng et al. (2016) compiled new and previously published suites of eastern Chinese speleothems that record the $\delta^{18}O$ of regional rainfall over the last 640,000 years. The composite record was dated using over 200 U–Th ages, as shown in FIGURE 4. The resulting Asian monsoon $\delta^{18}O$ record reveals that the timing of past changes in the Asian monsoon largely matches the timing of Northern Hemisphere solar insolation cycles (FIG. 4). This finding supports the theory that Northern Hemisphere insolation acts as an important pacemaker of the monsoon. The Asian monsoon $\delta^{18}O$ record can be correlated to marine and ice core records, thereby elucidating the interplay between insolation, the cryosphere, sea levels, tropical rainfall, and greenhouse gases within and through glacial cycles. These intercomparisons, when placed on a robust chronology, shed important light on the mechanisms and sequence of events leading up to major swings in Earth's climate, such as the abrupt end, or termination, of a glacial period.

Climate Link to Chinese Dynasties

Focusing on the last two millennia, a high-resolution record of $\delta^{18}O$ from calcite within Wanxiang Cave can be compared directly to historical records in order to evaluate the climatic context of societal transformations in ancient civilizations (Zhang et al. 2008). For example, increased monsoon rainfall between AD 960 and AD 1020 may have contributed to the rapid increase in rice cultivation and a dramatic rise of population under the Northern Song Dynasty in China (FIG. 5). In contrast, the final decades of the Tang, Yuan, and Ming Dynasties—all characterized as periods of unrest—coincide with drier conditions. Further examination shows that the timing of Asian monsoon variability coincides with the retreat and advance of glaciers in the Swiss Alps, which relate to temperature in the European and North Atlantic regions (FIG. 5). The climatic link, or teleconnection, between these two distant locations has been well documented (see Wang et al. 2001). Indeed, the rainy and prosperous period in China between 960 and 1020 coincides with warmer temperatures (the Medieval Climatic Optimum) in the North Atlantic realm, as evidenced by retreating alpine glaciers in Europe and the appearance of Viking colonies in Greenland. While a myriad of sociopolitical changes can ultimately contribute to societal change, the coincidence of events suggest that these ancient civilizations were likely influenced by abrupt shifts in their respective regional climates.

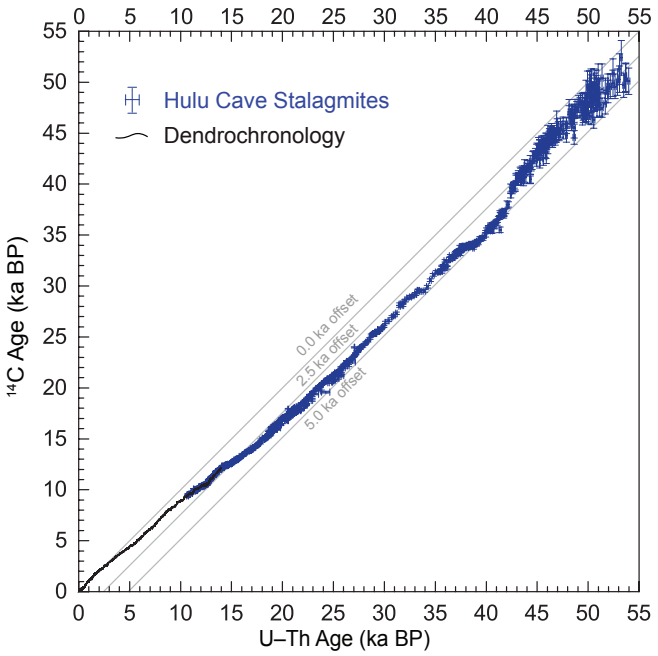

FIGURE 6 The U–Th ages versus ^{14}C ages of multiple stalagmites from Hulu Cave (near Nanjing, China) (blue) plotted with a portion of the dendrochronology part of the IntCal20 curve (black). The U–Th ages and ^{14}C ages are plotted with associated 2σ and 1σ uncertainties, respectively. The diagonal lines (gray) show the offset between ^{14}C ages and U–Th ages. FIGURE MODIFIED FROM CHENG ET AL. (2018); INTCAL20 DATA FROM REIMER ET AL. (2020).

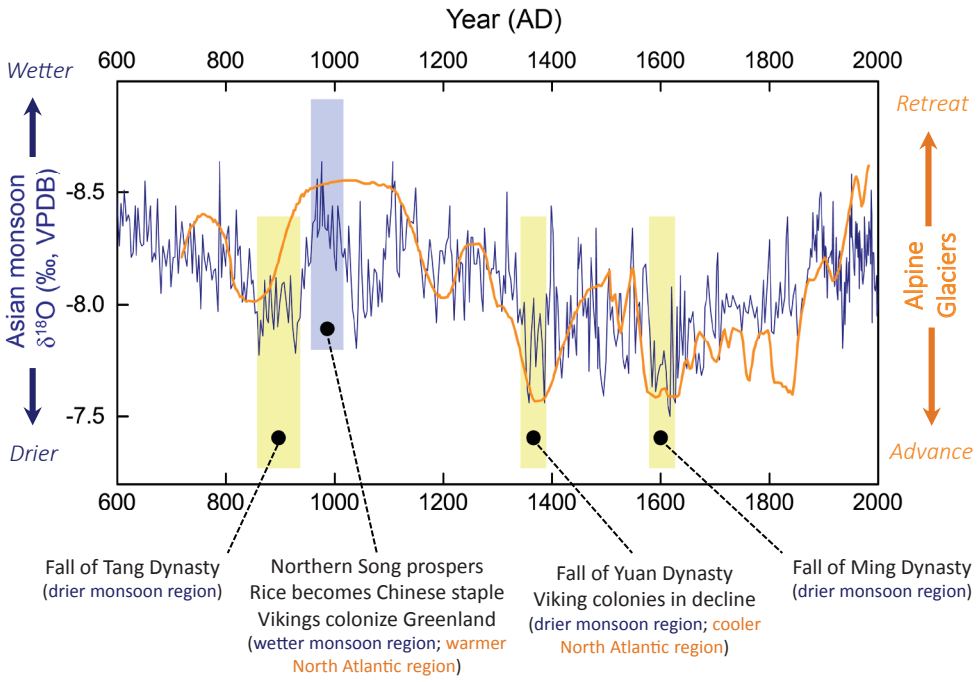

FIGURE 5 The $\delta^{18}O$ data from Wanxiang Cave (China) (blue) and the retreat and advance of European alpine glaciers (orange) between AD 600 and AD 2000. Dry periods in the Asian monsoon region coincide with glacial advance in Europe (vertical yellow bars); wet periods in the Asian monsoon region coincide with glacial retreat in Europe (vertical blue bar). Contemporaneous historical events are indicated. Abbreviation: VPDB = Vienna Pee Dee Belemnite. FIGURE MODIFIED FROM ZHANG ET AL. (2008); ALPINE GLACIER DATA FROM HOLZHAUSER ET AL. (2005).

Changes in Atmospheric $^{14}C/^{12}C$

Radiocarbon (^{14}C) dating is the cornerstone of several subdisciplines. Robust ^{14}C dating requires a firm understanding of changes in atmospheric $^{14}C/^{12}C$ over time. International ^{14}C calibration curves have been established using independently dated archives, such as tree rings, lacustrine and marine sediments, speleothems, and corals. Up until 2018, however, the older half of the curve was poorly constrained due to the lack of absolute-dated materials in this time range, which contain significant proportions of carbon derived from the atmosphere.

Stalagmites from Hulu Cave (eastern China) offer a resolution to this problem. The stalagmites are unique in that they display low and stable dead carbon fractions (see Cheng et al. 2018 for details). Measurements of $^{14}C/^{12}C$ ratios and ^{14}C ages can be paired directly with U–Th ages within the same stalagmite. The result is a seamless atmospheric $^{14}C/^{12}C$ record that covers much of the range of the radiocarbon dating method from a single source (FIG. 6). The Hulu $^{14}C/^{12}C$ record completes the full range of the radiocarbon calibration at a reasonable level of precision and has been incorporated in the new IntCal20 calibration (Reimer et al. 2020).

CONCLUSIONS

Speleothems represent a powerful archive of climate and environmental change. One of the great advantages of studying speleothems is that they can be accurately and precisely dated using U–Th methods from a few years to 650 ka. Key technical advancements over the last 35 years have led to vast improvements in analytical precision and reductions in sample size requirements. The U–Th dating of speleothems has led to major advances in several subfields of Quaternary sciences. In this review, we outlined the principles and history of U–Th dating of speleothems. In addition, we highlighted three speleothem studies that applied U–Th dating methods to investigate the timing of past Asian monsoon changes, the climatic context of ancient civilizations, and past changes in atmospheric $^{14}C/^{12}C$.

ACKNOWLEDGMENTS

This contribution was supported by the National Science Foundation (NSF) grants 1702816 and 1602940, and the Austrian Science Foundation (FWF) grant P327510. We thank reviewers D.A. Richards and W.D. Sharp and all 3 editors for their constructive feedback, which improved this manuscript considerably.

REFERENCES

Bateman H (1910) The solution of a system of differential equations occurring in the theory of radioactive transformations. Proceedings of the Cambridge Philosophical Society, Mathematical and Physical Sciences 15: 423-427

Barnes JW, Lang EJ Potratz HA (1956) Ratio of ionium to uranium in coral limestone. Science 124: 175-176, doi: 10.1126/science.124.3213.175-a

Buizert C and 16 coauthors (2015) The WAIS Divide deep ice core WD2014 chronology – Part 1: methane synchronization (68–31 ka BP) and the gas age–ice age difference. Climate of the Past 11: 153-173, doi: 10.5194/cp-11-153-2015

Chen JH, Edwards RL, Wasserburg GJ (1986) ^{238}U,^{234}U and ^{232}Th in seawater. Earth and Planetary Science Letters 80: 241-251, doi: 10.1016/0012-821X(86)90108-1

Cheng H, Adkins J, Edwards RL, Boyle EA (2000) U-Th dating of deep-sea corals. Geochimica et Cosmochimica Acta 64: 2401-2416, doi: 10.1016/S0016-7037(99)00422-6

Cheng H and 11 coauthors (2013) Improvements in ^{230}Th dating, ^{230}Th and ^{234}U half-life values, and U–Th isotopic measurements by multi-collector inductively coupled plasma mass spectrometry. Earth and Planetary Science Letters 371-372: 82-91, doi: 10.1016/j.epsl.2013.04.006

Cheng H and 13 coauthors (2016) The Asian monsoon over the past 640,000 years and ice age terminations. Nature 534: 640-646, doi: 10.1038/nature18591

Cheng H and 14 coauthors (2018) Atmospheric $^{14}C/^{12}C$ changes during the last glacial period from Hulu Cave. Science 362: 1293-1297, doi: 10.1126/science.aau0747

Cherdyntsev VV (with Chalov PI and others) (1955) Transactions of the Third Session of the Commission for Determining the Absolute Age of Geological Formations. Izvestiya Akademii Nauk, Seriya Geologicheskaya, SSSR, Moscow: 175-182 (In Russian)

Edwards RL, Chen JH, Wasserburg GJ (1987) ^{238}U–^{234}U–^{230}Th–^{232}Th systematics and the precise measurement of time over the past 500,000 years. Earth and Planetary Science Letters 81: 175-192, doi: 10.1016/0012-821X(87)90154-3

Edwards RL (1988) High precision thorium-230 ages of corals and the timing of sea level fluctuations in the late Quaternary. PhD thesis, California Institute of Technology, 367 pp, doi: 10.7907/S2FW-0463

Edwards RL, Taylor FW, Wasserburg GJ (1988) Dating earthquakes with high-precision thorium-230 ages of very young corals. Earth and Planetary Science Letters 90: 371-381, doi: 10.1016/0012-821X(88)90136-7

Edwards RL, Cheng H, Murrell MT, Goldstein SJ (1997) Protactinium-231 dating of carbonates by thermal ionization mass spectrometry: implications for Quaternary climate change. Science 276: 782-786, doi: 10.1126/science.276.5313.782

Hellstrom J (2006) U–Th dating of speleothems with high initial ^{230}Th using stratigraphical constraint. Quaternary Geochronology 1: 289-295, doi: 10.1016/j.quageo.2007.01.004

Holzhauser H, Magny M, Zumbuühl HJ (2005) Glacier and lake-level variations in west-central Europe over the last 3500 years. The Holocene 15: 789-801, doi: 10.1191/0959683605hl853ra

Ivanovich M, Harmon RS (eds) (1982) Uranium Series Disequilibrium: Applications to Environmental Problems. Clarendon Press, Oxford, 571 pp

Johnson (2021) Tales from the underground: speleothem records of past hydroclimate. Elements 17: 93-100

Jaffey AH, Flynn KF, Glendenin LE, Bentley WC, Essling AM (1971) Precision measurement of half-lives and specific activities of ^{235}U and ^{238}U. Physical Review C 4: 1889-1906, doi: 10.1103/PhysRevC.4.1889

Kaufman A, Broecker WS (1965) Comparison of Th^{230} and C^{14} ages for carbonate materials from lakes Lahontan and Bonneville. Journal of Geophysical Research 70: 4039-4054, doi: 10.1029/JZ070i016p04039

Li X and 5 coauthors (2021) Novel method for determining of ^{234}U–^{238}U ages from Devils Hole 2 cave calcite (Nevada). Geochronology 3: 49-58, doi: 10.5194/gchron-3-49-2021

Reimer PJ and 41 coauthors (2020) The IntCal20 Northern Hemisphere radiocarbon age calibration curve (0–55 cal kBP). Radiocarbon 62: 1-33, doi: 10.1017/RDC.2020.41

Richards DA, Dorale JA (2003) Uranium-series chronology and environmental applications of speleothems. Reviews in Mineralogy and Geochemistry 52: 407-460, doi: 10.2113/0520407

Richards DA, Andersen MB (2013) Time constraints and tie-points in the Quaternary Period. Elements 9: 45-51, doi: 10.2113/gselements.9.1.45

Rosholt JN, Antal PS (1962) Evaluation of the $^{231}Pa/U$-$^{230}Th/U$ method for dating Pleistocene carbonate rocks. Geological Survey Research 1962: Short Papers in Geology, Hydrology and Topography, Articles 180-239. US Geological Survey Professional Paper 450-E, United States Government Printing Office. Article 209, pp E108-E111, doi: 10.3133/pp450E

Rutherford E, Soddy F (1902) The cause and nature of radioactivity.—Part II. Philosophical Magazine, Series 6: 569-585, doi: 10.1080/14786440209462881

Thurber DL, Broecker WS, Blanchard RL, Potratz HA (1965) Uranium-series ages of Pacific atoll coral. Science 149: 55-58, doi: 10.1126/science.149.3679.55

Wang YJ and 6 authors (2001) A high-resolution absolute-dated late Pleistocene monsoon record from Hulu Cave, China. Science 294: 2345-2348, doi: 10.1126/science.1064618

Wendt KA and 5 coauthors (2020) Paleohydrology of southwest Nevada (USA) based on groundwater $^{234}U/^{238}U$ over the last 475 k.y. Geological Society of America Bulletin 132: 793-802, doi: 10.1130/B35168.1

Woodhead J and 5 coauthors (2012) U and Pb variability in older speleothems and strategies for their chronology. Quaternary Geochronology 14: 105-113, doi: 10.1016/j.quageo.2012.02.028

Zhang P and 16 coauthors (2008) A test of climate, sun, and culture relationships from an 1810-year Chinese cave record. Science 322: 940-942, doi: 10.1126/science.1163965 ■